

Article

Quantum Advantages of Teleportation and Dense Coding Protocols in an Open System

Saeed Haddadi ^{1,2}, Maryam Hadipour ³, Soroush Haseli ^{1,3}, Atta Ur Rahman ⁴ and Artur Czerwinski ^{5,*}

¹ School of Physics, Institute for Research in Fundamental Sciences (IPM), Tehran P.O. Box 19395-5531, Iran; saeed@ssqig.com (S.H.); soroush.haseli@uut.ac.ir (S.H.)

² Saeed's Quantum Information Group, Tehran P.O. Box 19395-0560, Iran

³ Faculty of Physics, Urmia University of Technology, Urmia 57166-93188, Iran; maryam.hadipour@sci.uut.ac.ir

⁴ School of Physics, University of Chinese Academy of Sciences, Yuquan Road 19A, Beijing 100049, China; a.rahman@whu.edu.cn

⁵ Institute of Physics, Faculty of Physics, Astronomy and Informatics, Nicolaus Copernicus University in Torun, Ul. Grudziadzka 5, 87-100 Torun, Poland

* Correspondence: aczerwin@umk.pl

Abstract: Quantum teleportation and dense coding are well-known quantum protocols that have been widely explored in the field of quantum computing. In this paper, the efficiency of quantum teleportation and dense coding protocols is examined in two-level atoms with two-photon transitions via the Stark shift effect, where each atom is separately coupled to a dissipative reservoir at zero temperature. Our results show that non-Markovianity and Stark shift can play constructive roles in restoring the quantum advantages of these protocols after they are diminished. These findings could offer a potential solution to preserving the computational and communicative advantages of quantum technologies.

Keywords: Stark effect; teleportation; dense coding; non-Markovianity; open systems; storing

MSC: 81P45; 81P47; 81P48



Citation: Haddadi, S.; Hadipour, M.; Haseli, S.; Rahman, A.U.; Czerwinski, A. Quantum Advantages of Teleportation and Dense Coding Protocols in an Open System. *Mathematics* **2023**, *11*, 1407. <https://doi.org/10.3390/math11061407>

Academic Editor: Jonathan Blackledge

Received: 11 February 2023

Revised: 9 March 2023

Accepted: 13 March 2023

Published: 14 March 2023



Copyright: © 2023 by the authors. Licensee MDPI, Basel, Switzerland. This article is an open access article distributed under the terms and conditions of the Creative Commons Attribution (CC BY) license (<https://creativecommons.org/licenses/by/4.0/>).

1. Introduction

Quantum communication protocols have special quantum advantages, such as security and high capacity, compared to their classical counterparts [1–4]. Among the various quantum communication protocols, quantum teleportation is an old protocol that uses the initial entanglement between Alice as the sender and Bob as the receiver [5]. In quantum teleportation protocols, the transmission of a desired state is possible using local operations and classical communication. If Alice and Bob share a maximally entangled channel state, then the fidelity value between the sending and receiving states will be equal to unity under ideal conditions [5]. The quantum teleportation protocol has the quantum advantage when the value of the average fidelity is greater than its classical bound, which is equal to $2/3$ [6,7]. Moreover, some authors [8,9] proved that the optimal teleportation fidelity f_{\max} is a linear function $f_{\max} = (2\mathcal{F}_{\max} + 1)/3$ of the maximal singlet fraction or fidelity \mathcal{F}_{\max} defined as the maximal overlap of a state with a maximally entangled state.

Another quantum communication protocol that is designed based on sharing entanglement between the sender and receiver is known as quantum dense coding [10–12]. In quantum dense coding protocols, one qubit is sent from the sender to the receiver, and two bits of classical information are transmitted through this protocol if the state of the channel is maximally entangled. It is worth mentioning that this protocol can still show a quantum advantage even if the initial channel state is not maximally entangled [13].

The quantum advantage of quantum teleportation and dense coding protocol entirely depends on the initial entanglement shared between the sender and the receiver [14–17].

The initial entanglement between the sender and the receiver can be reduced and destroyed under the effect of the external environment [18]. Therefore, the influence of different environmental noises on quantum teleportation [19–23] and dense coding protocols [24–28] has been given special attention. Various methods have been introduced to protect the quantum advantages of the mentioned protocols under quantum noise, such as choosing the appropriate initial state of the channel [29,30], using different structures for noise [31,32], applying filter operations [33], and weak measurements [34,35].

In the real world, it is difficult and almost impossible to isolate the system from its surroundings. So, the interaction of the system with the environment is almost an inevitable phenomenon. In quantum information theory, the topic of open quantum systems has received much attention [36–41]. In general, determining the evolution of a quantum system that interacts with its surroundings is a complex and difficult process. According to the type of interaction of the system with its environment, the dynamics of open quantum systems are divided into two categories: Markovian and non-Markovian. In Markovian dynamics, information continuously flows from the system to the environment. However, in the non-Markovian dynamical transformation, in some time intervals, the information flows back to the system from the environment [42–44]. The dynamics of quantum correlations in open quantum systems has been the subject of many recent types of research [45–52]. Due to the interaction of the quantum system with the environment, quantum correlations in quantum systems are changed, and in general, they are quickly destroyed. The behavior of quantum correlations in open quantum systems depends on the type of evolution of the quantum system. In general, the amount of quantum correlations in Markovian evolution is continuously reduced and destroyed [53–55] while in non-Markovian evolution, quantum correlations are restored due to the presence of memory effects in some intervals and show fluctuating behavior [56–58]. Due to the importance of quantum correlations as a source in quantum information theory, several methods have been introduced to protect them against decoherence [59–62].

In reference [63], the process of excitation of the atomic two-photon, which is controlled by time-dependent quantum evolution, has been studied from the spectroscopic precision point of view. Furthermore, Stark shift dynamics calculated in two-compartment Coulomb systems show high efficiency in resonance ionization spectroscopy. The authors of reference [64] show how to regulate a spontaneous emission using dc field inside a cavity. The study of the Stark effect on the evolution of entanglement in quantum systems without considering the dissipation of the system has been the subject of some works [65,66].

Recently, Golkar and Tavassoly [67] revealed that the entanglement of a system consisting of two two-level atoms is protected using the Stark effect in a dissipative environment. Motivated by this, we consider quantum teleportation and dense coding in two-level atoms via two-photon transitions along with the Stark shift effect, in which each atom is coupled to a dissipative reservoir at zero temperature. We will focus on the efficiency of the Stark shift effect in Markovian and non-Markovian reservoirs for implementing quantum teleportation and dense coding protocols. Our results show that the effect of the Stark shift in the non-Markovian reservoir is useful for protecting the quantum advantages of teleportation and dense coding, implying that the complex effects of both Markovian and non-Markovian reservoirs on the quantum advantages of the mentioned protocols.

2. The Model and Its Solution

This section employs a physical model of an open quantum system in which two two-level atoms (two identical qubits) interact separately with two independent environments in the presence of the Stark effect at zero temperature (see Figure 1). Here, we briefly introduce the model used in this work. We assume that two qubits A and B interact independently and locally with two independent environments E_1 and E_2 , respectively, in the presence of the Stark effect at zero temperature [67]. In the presence of the Stark effect, this model can be considered as the interaction of a two-level system with its environment field due to two-photon transitions, viz

$$\begin{aligned} \hat{H}_{\text{eff}} = & \omega_0 (\hat{\sigma}_+^A \hat{\sigma}_-^A + \hat{\sigma}_+^B \hat{\sigma}_-^B) + \sum_{i_1} \omega_{i_1} \hat{a}_{i_1}^\dagger \hat{a}_{i_1} + \sum_{i_2} \omega_{i_2} \hat{a}_{i_2}^\dagger \hat{a}_{i_2} \\ & + \sum_{i_1} g_{i_1} (\hat{a}_{i_1}^{\dagger 2} \hat{\sigma}_-^A + \hat{a}_{i_1}^2 \hat{\sigma}_+^A) + \sum_{i_1} \hat{a}_{i_1}^\dagger \hat{a}_{i_1} (\beta_{i_1} \hat{\sigma}_-^A \hat{\sigma}_+^A + \eta_{i_1} \hat{\sigma}_+^A \hat{\sigma}_-^A) \\ & + \sum_{i_2} g_{i_2} (\hat{a}_{i_2}^{\dagger 2} \hat{\sigma}_-^B + \hat{a}_{i_2}^2 \hat{\sigma}_+^B) + \sum_{i_2} \hat{a}_{i_2}^\dagger \hat{a}_{i_2} (\beta_{i_2} \hat{\sigma}_-^B \hat{\sigma}_+^B + \eta_{i_2} \hat{\sigma}_+^B \hat{\sigma}_-^B), \end{aligned} \tag{1}$$

where the environment modes have frequencies ω_j ($j = 1, 2$), respectively associated with E_1 and E_2 . Moreover, ω_0 is the transition frequency of the two qubits, $\hat{a}_{i_j}^\dagger$ (\hat{a}_{i_j}) is the creation (annihilation) operator of the i th mode of the j th environment, and $\hat{\sigma}_+^P$ ($\hat{\sigma}_-^P$) with $P \in \{A, B\}$ is the raising (lowering) operator for qubit P . Moreover, g_{i_1} and g_{i_2} are the coupling constant between the qubits and environments and the parameters β_{i_j} and η_{i_j} are the Stark shift coefficients [68]. It is appropriate to continue the work in the interaction picture. So, the above effective Hamiltonian in the interaction picture will be written as follows

$$\begin{aligned} \hat{H}_{\text{int}} = & \sum_{i_1} g_{i_1} (\hat{a}_{i_1}^{\dagger 2} \hat{\sigma}_-^A e^{-i(\omega_0 - 2\omega_{i_1})t} + \hat{a}_{i_1}^2 \hat{\sigma}_+^A e^{i(\omega_0 - 2\omega_{i_1})t}) + \sum_{i_1} \hat{a}_{i_1}^\dagger \hat{a}_{i_1} (\beta_{i_1} \hat{\sigma}_-^A \hat{\sigma}_+^A + \eta_{i_1} \hat{\sigma}_+^A \hat{\sigma}_-^A) \\ & + \sum_{i_2} g_{i_2} (\hat{a}_{i_2}^{\dagger 2} \hat{\sigma}_-^B e^{-i(\omega_0 - 2\omega_{i_2})t} + \hat{a}_{i_2}^2 \hat{\sigma}_+^B e^{i(\omega_0 - 2\omega_{i_2})t}) + \sum_{i_2} \hat{a}_{i_2}^\dagger \hat{a}_{i_2} (\beta_{i_2} \hat{\sigma}_-^B \hat{\sigma}_+^B + \eta_{i_2} \hat{\sigma}_+^B \hat{\sigma}_-^B). \end{aligned} \tag{2}$$

Let us assume that the initial state of the system (qubit environment) is as follows

$$|\psi(0)\rangle = (\mu|0\rangle_A |1\rangle_B + \sqrt{1 - \mu^2}|1\rangle_A |0\rangle_B) \otimes |0_{i_1}\rangle_{E_1} |0_{i_2}\rangle_{E_2}, \tag{3}$$

where $\mu \in [0, 1]$, $|0_{i_j}\rangle_{E_j}$ is the vacuum state of the j th environment, and $|0\rangle_P$ ($|1\rangle_P$) is the ground (excited) state of the two qubits. Considering that the number of excitations in the total system is preserved, the dynamics of the whole system at an arbitrary time $t > 0$ can be obtained as follows

$$\begin{aligned} |\psi(t)\rangle = & (c_1(t)|1\rangle_A |0\rangle_B + c_2(t)|0\rangle_A |1\rangle_B) |0_{i_1}\rangle_{E_1} |0_{i_2}\rangle_{E_2} \\ & + \sum_{i_1} c_{i_1}(t) |0\rangle_A |0\rangle_B |2_{i_1}\rangle_{E_1} |0_{i_2}\rangle_{E_2} \\ & + \sum_{i_2} c_{i_2}(t) |0\rangle_A |0\rangle_B |0_{i_1}\rangle_{E_1} |2_{i_2}\rangle_{E_2}. \end{aligned} \tag{4}$$

Above, $|2_{i_j}\rangle_{E_j}$ indicates that there exist two photons in the mode i of the j th environment. Using the time-dependent Schrödinger equation $\hat{H}_{\text{int}}|\psi(t)\rangle = i(\partial/\partial t)|\psi(t)\rangle$, the coupled equations for amplitude probability will be obtained as follows

$$\dot{c}_j(t) = -i\sqrt{2} \sum_{i_j} g_{i_j} c_{i_j}(t) e^{i(\omega_0 - \omega_{i_j})t}, \tag{5}$$

$$\dot{c}_i(t) = -i\sqrt{2} g_{i_j}^* c_j(t) e^{-i(\omega_0 - \omega_{i_j})t} - 2i\beta_{i_j} c_{i_j}(t). \tag{6}$$

By observing the Schrödinger equation and attempting to solve it for the defined model, we find that the terms $\eta_{i_1} \hat{a}_{i_1}^\dagger \hat{a}_{i_1} \hat{\sigma}_+^A \hat{\sigma}_-^A |\psi(t)\rangle$ and $\eta_{i_2} \hat{a}_{i_2}^\dagger \hat{a}_{i_2} \hat{\sigma}_+^B \hat{\sigma}_-^B |\psi(t)\rangle$ are equal to zero. Hence, the parameters η_{i_1} and η_{i_2} will not play a role in the evolution of the quantum system. By performing mathematical calculations and integrating Equation (6) and finally putting its result in Equation (5), we will reach an integro-differential equation as

$$\dot{c}_j(t) = -2 \int_0^t dt' f(t - t') c_j(t'), \tag{7}$$

where $f(t - t')$ is the correlation function and has the following form

$$f(t - t') = \int d\omega_i J(\omega_i) \exp[i(\omega_0 - 2\omega_i - 2\beta)(t - t')]. \tag{8}$$

Here, it is supposed that $\beta_{i_1} = \beta_{i_2} = \beta$ and $\omega_{i_1} = \omega_{i_2} = \omega_i$. On the scale of a large number of environmental modes, the sum of the modes can be converted into an integral as $\sum_i |g_i|^2 \rightarrow \int d\omega_i J(\omega_i)$, in which $J(\omega_i)$ represents the spectral density of the electromagnetic field inside the dissipative cavity. In our work, it is assumed that the spectral density of the environment has a Lorentzian form as [36]

$$J(\omega_i) = \frac{1}{2\pi} \frac{\gamma_0 \lambda^2}{(\omega_0 - 2\omega_i)^2 + \lambda^2}, \tag{9}$$

where λ shows the spectral width of the environment and is related to the environment's correlation time $\tau_\mathcal{E} \approx 1/\lambda$. It can be shown that the parameter γ_0 is connected to the decay rate of the excited state of the atom. It should also be noted that the relaxation time scale τ_s over which the system changes depends on the parameter γ_0 through $\tau_s \approx 1/\gamma_0$ [69]. By using the Lorentzian spectral density in Equation (9) and inserting it into Equation (8), the correlation function takes the following form

$$f(t - t') = \frac{\gamma_0 \lambda}{2} \exp[-(\lambda + 2i\beta)(t - t')]. \tag{10}$$

By making use of this correlation function and applying the Laplace transformation to solve the integro-differential equation in Equation (7), the exact solutions for $c_1(t)$ and $c_2(t)$ can be obtained as

$$c_1(t) = \mu \varepsilon(t), \quad c_2(t) = \sqrt{1 - \mu^2} \varepsilon(t), \tag{11}$$

where

$$\varepsilon(t) = e^{-\frac{(\lambda + 2i\beta)t}{2}} \left[\cosh\left(\frac{\Omega t}{2}\right) + \frac{\lambda + 2i\beta}{\Omega} \sinh\left(\frac{\Omega t}{2}\right) \right], \tag{12}$$

with

$$\Omega = \sqrt{-4\gamma_0 \lambda + (\lambda + 2i\beta)^2}. \tag{13}$$

In the usual basis $\{|1_A, 1_B\rangle, |1_A, 0_B\rangle, |0_A, 1_B\rangle, |0_A, 0_B\rangle\}$, the time-dependent reduced density matrix is written as follows [67]

$$\rho_t = \begin{pmatrix} 0 & 0 & 0 & 0 \\ 0 & \rho_{22} & \rho_{23} & 0 \\ 0 & \rho_{23}^* & \rho_{33} & 0 \\ 0 & 0 & 0 & \rho_{44} \end{pmatrix}, \tag{14}$$

where $\rho_{22} = |c_1(t)|^2$, $\rho_{23} = c_1(t)c_2^*(t)$, $\rho_{33} = |c_2(t)|^2$ and $\rho_{44} = -\rho_{22} - \rho_{33} + 1$.

The model used in this work can be applied to two different regimes: weak and strong coupling regimes [70]. In a weak coupling regime, the relaxation time τ_s is greater than the environment correlation time $\tau_\mathcal{E}$, i.e., $\tau_s > 2\tau_\mathcal{E}$ and $\gamma_0 < \lambda/2$. In this regime, the dynamics of the quantum system are Markovian, and a decay process occurs during time evolution. While the situation is different in the strong coupling regime. In a strong coupling regime the environment correlation time $\tau_\mathcal{E}$ is greater than the relaxation time of the system τ_s , namely $\tau_s < 2\tau_\mathcal{E}$ and $\gamma_0 > \lambda/2$. In this regime, the dynamics are non-Markovian, and due to the memory effects, the revival of information with oscillations can be observed. In this paper, both the Markovian and non-Markovian regimes will be considered in the presence or absence of the Stark shift effect.

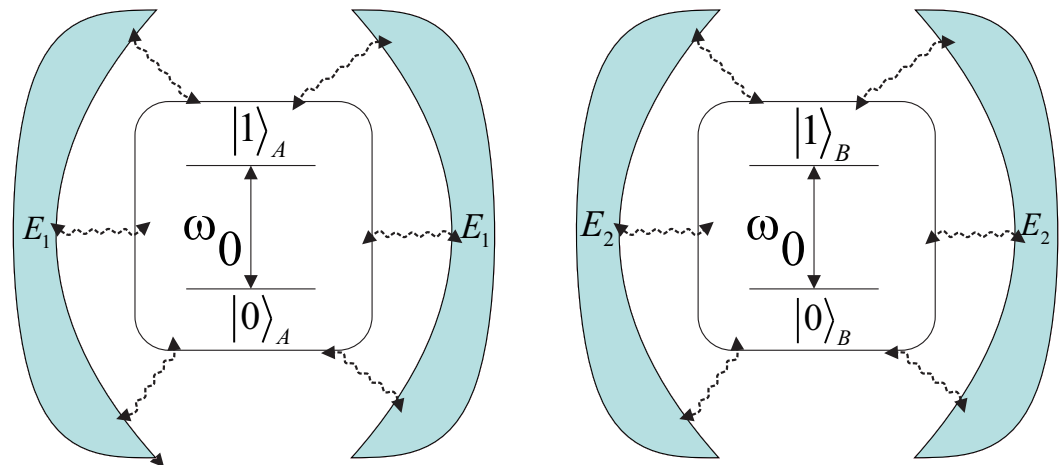


Figure 1. Schematic representation of two-level atoms *A* and *B*, which interact independently with their surrounding environments E_1 and E_2 respectively. There is no interaction between the two interacting subsystems $A - E_1$ and $B - E_2$.

3. Quantum Teleportation

An entangled mixed state can be considered a resource for studying quantum teleportation [14,71,72]. In this work, we will investigate the impact of the Stark shift on the possibility of quantum teleportation through the chosen model. Here, it is assumed that the initial input state is an unknown two-qubit state

$$|\psi_{in}\rangle = \cos(\theta/2)|10\rangle + e^{i\phi} \sin(\theta/2)|01\rangle, \quad \forall \quad 0 \leq \theta \leq \pi, \quad 0 \leq \phi \leq 2\pi. \quad (15)$$

In the process of quantum teleportation, an initial input state $\rho_{in} = |\psi_{in}\rangle\langle\psi_{in}|$ is mapped to an output replica state ρ_{out} through a mixed channel ρ_{ch} . So, from the mathematical point of view in quantum theory, it can be said that the mixed channel ρ_{ch} is a completely positive map. By using joint measurement and local unitary operations on input state ρ_{in} , the output replica state ρ_{out} can be obtained as

$$\rho_{out} = \sum_{i,j=0}^3 p_i p_j (\sigma^i \otimes \sigma^j) \rho_{in} (\sigma^i \otimes \sigma^j), \quad (16)$$

where $\sigma^0 = \mathbf{I}$ is identity matrix, $\sigma^{1,2,3}$'s are common Pauli matrices, and $p_i = \text{tr}(\eta_i \rho_{ch})$ is the probability that the mixed channel ρ_{ch} is one of the well-known Bell states

$$\eta_0 = |\Psi^-\rangle\langle\Psi^-|, \quad \eta_1 = |\Phi^-\rangle\langle\Phi^-|, \quad \eta_2 = |\Psi^+\rangle\langle\Psi^+|, \quad \eta_3 = |\Phi^+\rangle\langle\Phi^+|. \quad (17)$$

Here, the quantum channel ρ_{ch} is assumed to be the time-dependent reduced density matrix ρ_t in Equation (14), i.e., $\rho_{ch} = \rho_t$. Hence, the output state is given by

$$\rho_{out} = \begin{pmatrix} \tilde{\rho}_{11} & 0 & 0 & 0 \\ 0 & \tilde{\rho}_{22} & \tilde{\rho}_{23} & 0 \\ 0 & \tilde{\rho}_{23}^* & \tilde{\rho}_{33} & 0 \\ 0 & 0 & 0 & \tilde{\rho}_{44} \end{pmatrix}, \quad (18)$$

where

$$\begin{aligned} \tilde{\rho}_{11} &= \tilde{\rho}_{44} = (\rho_{22} + \rho_{33})\rho_{44}, \\ \tilde{\rho}_{22} &= \rho_{44}^2 \cos^2(\theta/2) + (\rho_{22} + \rho_{33})^2 \sin^2(\theta/2), \\ \tilde{\rho}_{33} &= \rho_{44}^2 \sin^2(\theta/2) + (\rho_{22} + \rho_{33})^2 \cos^2(\theta/2), \\ \tilde{\rho}_{23} &= 2e^{i\phi} \rho_{23}^2 \sin \theta. \end{aligned} \quad (19)$$

The concept of fidelity between the initial input state ρ_{in} and the output state ρ_{out} can be used to test the quality of the quantum teleportation process [73–76]. The fidelity is described as

$$\mathcal{F} = \left(\text{tr} \sqrt{\sqrt{\rho_{in}} \rho_{out} \sqrt{\rho_{in}}} \right)^2. \tag{20}$$

If the input and output states are completely orthogonal, the fidelity value is zero and the performance of the quantum teleportation process has not been optimal at all and it fails. If the fidelity is equal to one, quantum teleportation has the most efficiency, i.e., the input state is identical to the output state. If $0 < \mathcal{F} < 1$, it means that the quantum information is disturbed during the transition and the quantum teleportation is not complete. According to the model chosen in this work and doing a series of mathematical calculations, the fidelity between the input (15) and output (18) states is obtained as follows

$$\mathcal{F} = \frac{\sin^2 \theta}{2} \left[\rho_{44}^2 + 4\rho_{23}^2 - (\rho_{22} + \rho_{33})^2 \right] + (\rho_{22} + \rho_{33})^2. \tag{21}$$

In order to quantify the performance of the quantum teleportation process, the average fidelity of teleportation F_A is described as [77]

$$F_A := \frac{1}{4\pi} \int_0^{2\pi} d\phi \int_0^\pi d\theta \mathcal{F} \sin \theta. \tag{22}$$

Inserting Equation (21) into Equation (22), and taking the integral, we have

$$F_A = \frac{1}{3} \left[\rho_{44}^2 + 4\rho_{23}^2 + 2(\rho_{22} + \rho_{33})^2 \right]. \tag{23}$$

As it is clear from the above equation, the average fidelity depends on the parameters of the quantum channel $\rho_{ch} = \rho_t$.

If the average fidelity F_A is more than 2/3 (its value in the classical world), then it can be said that the transmission of the quantum state using the quantum protocol is more favorable than the classical protocols.

In Figure 2, we discuss the average fidelity of teleportation (23) for the different values of the Stark shift parameter β against the scaled time τ . We set the parameter $\mu = 1/\sqrt{2}$ and evaluate the dynamics of teleportation using F_A under both Markovian and non-Markovian regimes of the independent reservoirs. Initially, $F_A = 1$ ensures that the teleportation of the initial two-qubit state has been successful. However, it seems that the further evolution of F_A depends on the Stark shift parameter. For example, in Figure 2a, the degree of fidelity decreases for the decreasing strength of β . Generally, F_A accommodates the highest values when $\beta = 5\gamma_0$ and the lowest ones when $\beta = 0$. This shows that the performance of coupled reservoirs can be strengthened by increasing β to succeed in teleportation. Moreover, per the definition of the coupling strengths, revivals in the dynamics of F_A are witnessed. This suggests the trade-off of the attributes between state and coupled reservoirs. On the other hand, Figure 2b illustrates the dynamics of F_A when the configuration is assumed in a Markovian regime. This regime seems to be highly fatal for teleportation compared to that observed in the non-Markovian regime. Even for the highest Stark shift parameter, F_A slopes quickly enter the classical domain. Nonetheless, in the case of the non-Markovian regime, F_A sustains the quantum advantage just for $\beta \geq \gamma_0$. Unlikely, for $\beta < \gamma_0$, the average fidelity of teleportation quickly enters into the classical domain, i.e., $F_A < 2/3$. In comparison, the quantum advantage of teleportation is quickly lost in the Markovian regime for all values of β . Therefore, the Markovian reservoir should be avoided for more prolonged success in the teleportation of two qubits under the current situation.

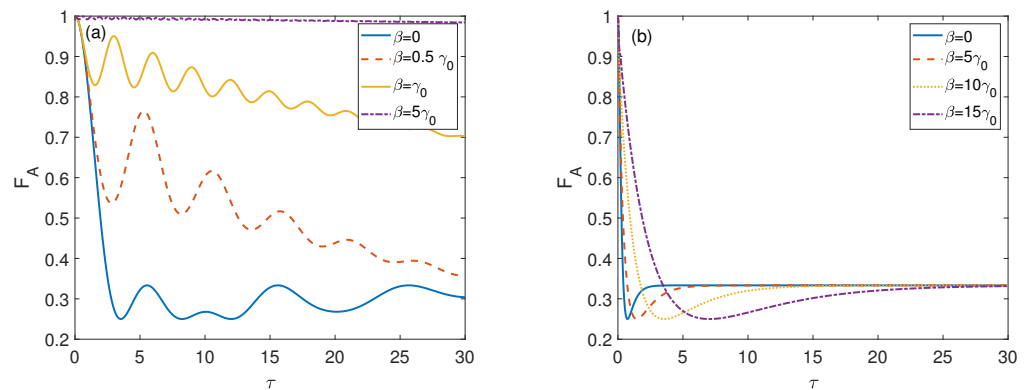


Figure 2. Average fidelity of teleportation (23) as a function of the scaled time $\tau = \gamma_0 t$ when $\mu = 1/\sqrt{2}$ for different values of Stark shift parameter β . (a) Non-Markovian regime with $\lambda = 0.1\gamma_0$ and (b) Markovian regime with $\lambda = 10\gamma_0$.

In Figure 3, we disclose the average fidelity dynamics of a two-qubit state when coupled with two independent reservoirs. Particularly, we focus on the average fidelity of teleportation for specific ranges of the Stark parameter β and scaled time $0 < \tau < 30$ when the reservoirs are assumed in a non-Markovian regime (Figure 3a) and in a Markovian regime (Figure 3b). Initially, we have $F_A = 1$. With time, the fidelity of the state continues to decrease, and the rate of decline seems to depend on the strength of the Stark shift parameter. As one can easily detect, for $\beta = \gamma_0$ in the non-Markovian regime, the state’s fidelity remains higher even for the prolonged scaled time. On the contrary, the fidelity of teleportation decreases with the decrease in the strength of β . We notice that the fidelity exhibits minimal values for $\beta = 0$. In comparison to the non-Markovian regime in Figure 3a, the fidelity remains weak when the coupling of the reservoirs is tuned to the Markovian regime. In this regime, the initial state’s teleportation degree is the same as that observed in the non-Markovian regime. However, with time, F_A shows a quicker loss and the teleportation protocol loses its quantum advantage compared to that observed under the non-Markovian regime, suggesting the beneficial nature of the reservoirs only in the non-Markovian regime. Moreover, in the non-Markovian regime, F_A stays in the quantum domain for $\beta > 0.5\gamma_0$ but quickly enters the classical domain for $\beta < 0.5\gamma_0$. In contrast, F_A quickly enters the classical domain for all values of the Stark shift parameter in the Markovian regime.

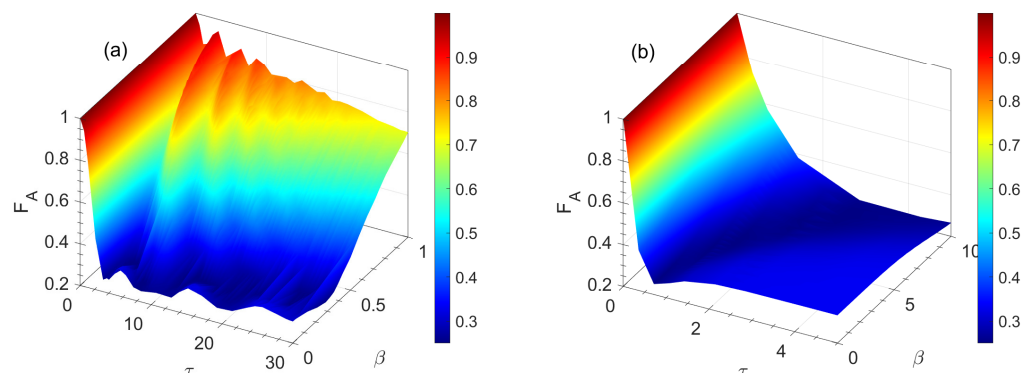


Figure 3. Average fidelity of teleportation in terms of the scaled time $\tau = \gamma_0 t$ and Stark shift parameter β for (a) non-Markovian $\lambda = 0.1\gamma_0$ and (b) Markovian $\lambda = 10\gamma_0$ regimes with $\mu = 1/\sqrt{2}$.

Figure 4 explores the average fidelity dynamics for the system of two qubits when exposed to two reservoirs influenced by the Stark shift effect. In the current case, we specifically focus on evaluating the role of a specific range of μ on the preservation of the average fidelity both in the Markovian and non-Markovian regimes. It is crucial to

note that we set λ to different values for the Markovian and non-Markovian reservoirs. In Figure 4a–c, we set the Stark shift parameter as $\beta = 0, 10\gamma_0,$ and $15\gamma_0,$ respectively, with $\lambda = 10\gamma_0.$ In these plots, for $\mu = 0.5,$ the fidelity of the state remains maximal and for all the other values of $\mu,$ it reduces from 1. On the other hand, in Figure 4d–f, we demonstrate the fidelity of the state when the reservoirs are considered in the non-Markovian regime. We notice that the initial value of the fidelity remains the same as that witnessed in Figure 4a–c. However, the associated qualitative dynamical map of the fidelity becomes different, where evident oscillations are observed. Note that at certain time intervals, fidelity is maintained in this regime and the teleportation protocol keeps its quantum advantage. As can be seen, the fidelity of teleportation stays in the quantum domain in the non-Markovian regime compared to that recorded in the Markovian regime. Hence, for successful and higher-order teleportation, one must tune the reservoirs to the non-Markovian reservoir.

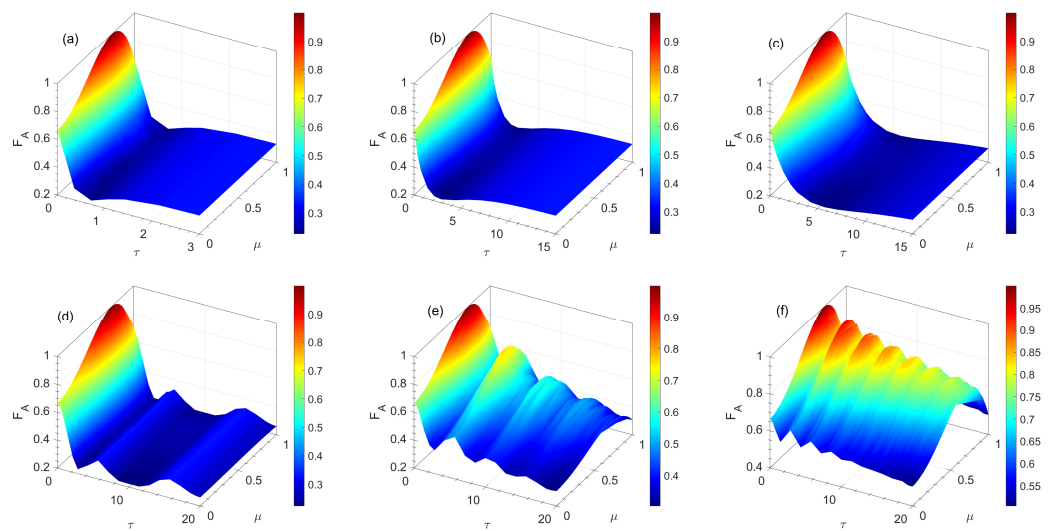


Figure 4. Average fidelity of teleportation versus the scaled time $\tau = \gamma_0 t$ and parameter μ for different values of the Stark shift parameter β in the Markovian regime [(a) $\beta = 0,$ (b) $\beta = 10\gamma_0,$ and (c) $\beta = 15\gamma_0$] with $\lambda = 10\gamma_0$ and in non-Markovian regime [(d) $\beta = 0,$ (e) $\beta = 0.5\gamma_0,$ and (f) $\beta = \gamma_0$] with $\lambda = 0.1\gamma_0.$

4. Quantum Dense Coding

In this section, we want to review the notion of quantum dense coding. It should be noted here that, unlike the quantum teleportation process, there is no need to physically send the quantum state in the dense coding process. Contrary to what happens in the quantum teleportation process, in the quantum dense coding, the transmission of the quantum state to a receiver will be done after applying local unitary transformation by the sender. The main goal of this process is to determine how much the quantum advantage of bipartite state ρ_{AB} is for transmitting classical information. The analytical formula of quantum dense coding protocol can be determined by the Holevo quantity as [13,78]

$$\chi(\rho_{AB}) := S(\bar{\rho}_{AB}) - S(\rho_{AB}), \tag{24}$$

where $\bar{\rho}_{AB} = \frac{1}{4} \sum_{i=0}^3 (\sigma^i \otimes \mathbf{I}) \rho_{AB} (\sigma^i \otimes \mathbf{I})$ denotes the signal ensemble average state and $S(\rho) = -\text{tr}(\rho \log_2 \rho)$ is the von Neumann entropy of the density matrix $\rho.$ Due to the fact that the Holevo quantity $\chi(\rho_{AB})$ is asymptotically available, it can be called the dense coding capacity [79]. Notice, we obtain the valid dense coding (quantum advantage) when $\chi(\rho_{AB}) > 1$ and for the optimal dense coding, we have $\chi(\rho_{AB})_{\max} = 2$ [80,81].

Based on the time-dependent density matrix (14), the average quantum state of the signal ensemble $\bar{\rho}_{AB}$ can be expressed as

$$\bar{\rho}_{AB} = \frac{1}{2} [\rho_{33}(|00\rangle\langle 00| + |10\rangle\langle 10|) + (1 - \rho_{33})(|01\rangle\langle 01| + |11\rangle\langle 11|)], \tag{25}$$

hence, the analytical expression of dense coding capacity (24) for our case (14) can be obtained as

$$\chi = -\rho_{33} \log_2 \frac{\rho_{33}}{2} - (1 - \rho_{33}) \log_2 \frac{1 - \rho_{33}}{2} + \rho_{44} \log_2 \rho_{44} + q^+ \log_2 q^+ + q^- \log_2 q^-, \quad (26)$$

where

$$q^\pm = \frac{1}{2} \left[(\rho_{22} + \rho_{33}) \pm \sqrt{(\rho_{22} - \rho_{33})^2 + 4|\rho_{23}|^2} \right].$$

The Holevo quantity (24), also known as the Holevo information, is a measure of the amount of classical information that can be transmitted using a quantum channel with a given set of quantum states. In the context of quantum dense coding, the Holevo quantity is used to quantify the maximum amount of classical information that can be transmitted by sending two quantum systems in a specific entangled state ρ_{AB} . This process allows the transmission of more information than would be possible with classical systems using the same amount of resources. The Holevo quantity can evaluate the performance of a quantum communication protocol and determine the optimal encoding strategy for a given set of quantum states.

In Figure 5, we present the dense coding capacity (26) as a function of the scaled time τ for different values of the Stark shift parameter β . We distinguish two scenarios: Markovian and non-Markovian environments. The key difference is that in the non-Markovian regime, the Holevo quantity features oscillations, which is a typical sign of memory effects. Consequently, over time, we have multiple local minima that result from the backflow of information. On the other hand, for Markovian dynamics, we witness a significant decline in the dense coding capacity and, soon after, the Holevo quantity increases and converges to an equilibrium value (valid dense coding when $\chi \rightarrow 1$), which is the same for all values of the Stark shift parameter.

Furthermore, in Figure 6, we observe the dense coding capacity versus time and the Stark shift parameter. In the strong coupling regime, the properties of the plot are more complex due to memory effects. In the strong coupling regime, the dynamics of the quantum system are non-Markovian, meaning that the system is affected by memory effects. In this regime, the Holevo quantity oscillates and revives over time, which indicates that there is a periodic exchange of information between the system and its environment.

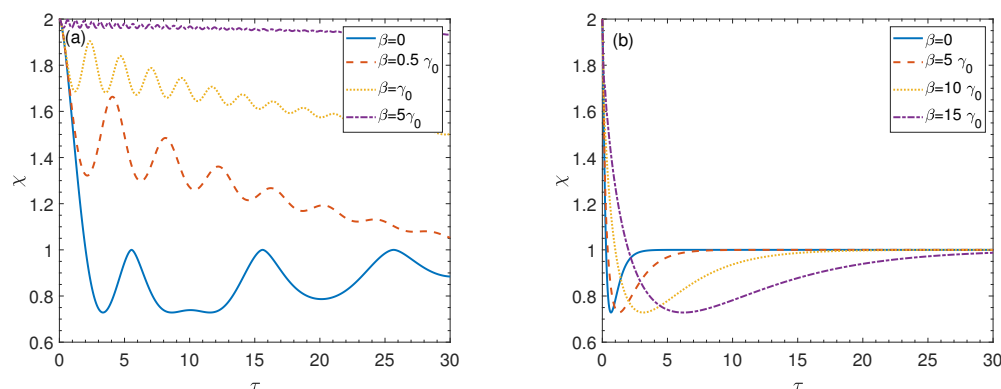


Figure 5. Dense coding capacity (26) as a function of the scaled time $\tau = \gamma_0 t$ when $\mu = 1/\sqrt{2}$ for different values of Stark shift parameter β . (a) Non-Markovian regime with $\lambda = 0.1\gamma_0$ and (b) Markovian regime with $\lambda = 10\gamma_0$.

In addition, in Figure 6a, there is an increase of the Holevo quantity with the Stark shift parameter, which can be interpreted as a result of the increased coherence between the two-level atoms and the environment, which leads to more efficient transmission of classical information. The Stark shift is a type of energy shift that can be caused by an external electric field, and it can affect the energy levels of a two-level atom. As the Stark shift parameter increases, the energy levels of the atoms become more separated, which

leads to a larger energy gap between the levels and a corresponding increase in coherence. In Figure 6b, the dense coding protocol loses its quantum advantage after a short period of time but regains it over time ($\chi \approx 1$) for small values of Stark shift.

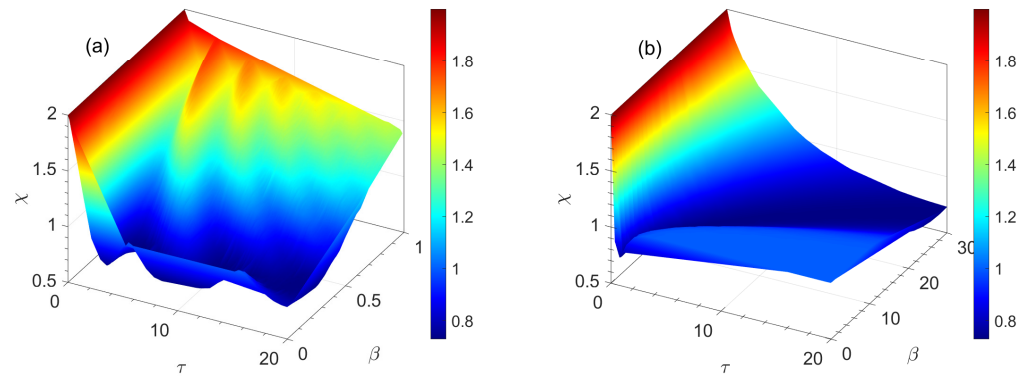


Figure 6. Dense coding capacity in terms of the scaled time $\tau = \gamma_0 t$ and Stark shift parameter β for (a) non-Markovian $\lambda = 0.1\gamma_0$ and (b) Markovian $\lambda = 10\gamma_0$ regimes with $\mu = 1/\sqrt{2}$.

In Figure 7, we observe the dense coding quantity versus time and the parameter μ , in Markovian and non-Markovian regimes, for different values of the Stark shift parameter, β . In the non-Markovian scenario, as the Stark shift parameter increases, the amplitude of the oscillations of the Holevo quantity declines. This can be understood again by considering that the Stark effect can be thought of as a shift in the energy levels of the two-level system. As the Stark shift parameter increases, the energy gap between the levels increases, which in turn leads to a decrease in the coupling between the system and its environment, resulting in a decrease in the amplitude of the oscillations of the Holevo quantity. In this figure, for the Markovian regime, we see that the maximum of the dense coding quantity declines as we increase the Stark shift parameter. This is due to the fact that in a Markovian regime, the system’s dynamics are governed by a decay process, and as the Stark shift parameter increases, the coupling between the system and its environment becomes stronger, leading to a faster decay of the system’s coherence and a decrease in the Holevo quantity.

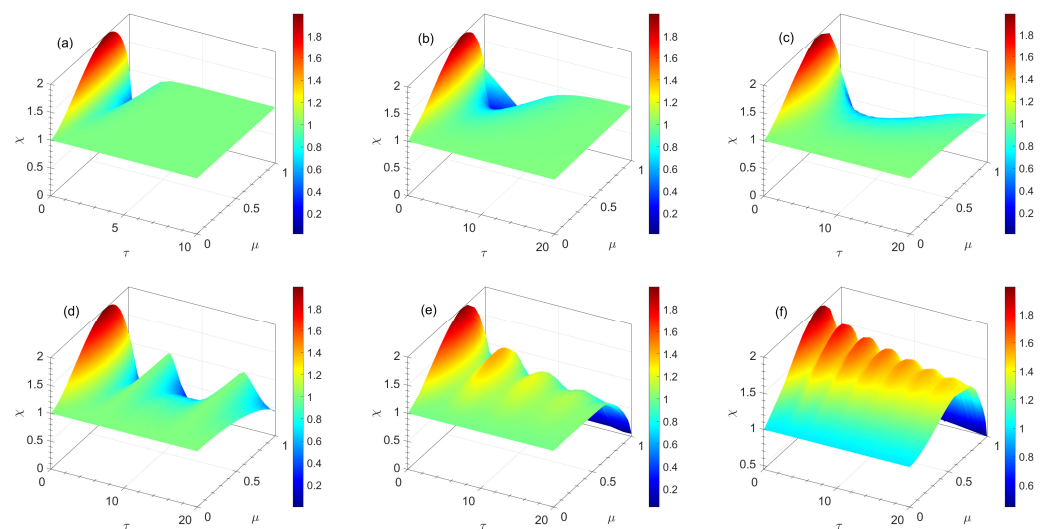


Figure 7. Dense coding capacity versus scaled time $\tau = \gamma_0 t$ and parameter μ for different values of Stark shift parameter β in Markovian regime [(a) $\beta = 0$, (b) $\beta = 10\gamma_0$, and (c) $\beta = 15\gamma_0$] with $\lambda = 10\gamma_0$ and in non-Markovian regime [(d) $\beta = 0$, (e) $\beta = 0.5\gamma_0$, and (f) $\beta = \gamma_0$] with $\lambda = 0.1\gamma_0$.

Overall, the results in Figures 5–7 suggest that the dynamics of quantum systems in the presence of the Stark effect can be highly dependent on the strength of the coupling

between the system and its environment as well as the Stark shift parameter. In the non-Markovian regime, memory effects lead to oscillations in the Holevo quantity, which can be used as a measure of the amount of classical information that can be transmitted using a quantum channel with a given set of quantum states. Furthermore, the results suggest that the Stark shift parameter can affect the coherence of the system and the efficiency of the quantum communication protocols. The increase of the Stark shift parameter leads to more efficient transmission of classical information in the strong coupling regime, but it also leads to a decrease in the amplitude of the oscillations of the Holevo quantity. In the Markovian regime, the Stark shift parameter leads to a faster decay of the system's coherence and a decrease in the Holevo quantity. These findings can be useful for designing and optimizing quantum communication protocols, particularly in the context of dense coding and quantum teleportation.

5. Concluding Remarks

We analyzed the efficiency of quantum teleportation and dense coding protocols for two identical qubits independently coupled to a dissipative reservoir at zero temperature in the presence of the Stark shift effect. Generally, we showed that the average fidelity of teleportation and the dense coding capacity are controllable by the Stark shift effect and the state parameter. In particular, we obtained the valid areas of these parameters where the examined protocols exhibited quantum advantages. Notably, we found that the Stark shift has a constructive impact on quantum advantages for both Markovian and non-Markovian reservoirs. However, this positive influence can be more evident in the non-Markovian reservoir even for lower Stark shift parameter values. Thereby, we believe that our results may provide a way to preserve the quantum advantages of the communication protocols in experiments involving quantum information-processing tasks. Of course, we considered only a physical model of an open quantum system where two identical qubits interact independently with two environments. For the other models with different reservoirs, it is still necessary to study more details.

Author Contributions: Conceptualization, all authors; methodology, S.H. (Soroush Haseli); software, S.H. (Soroush Haseli) and S.H. (Saeed Haddadi); validation, all authors; formal analysis, S.H. (Saeed Haddadi) and A.C.; investigation, all authors; resources, S.H. (Saeed Haddadi), S.H. (Soroush Haseli) and M.H.; writing—original draft preparation, all authors; writing—review and editing, S.H. (Saeed Haddadi) and A.C.; supervision, S.H. (Saeed Haddadi) and A.C.; project administration, S.H. (Saeed Haddadi) and A.C. All authors have read and agreed to the published version of the manuscript.

Funding: This research received no external funding.

Data Availability Statement: Not applicable.

Conflicts of Interest: The authors declare no conflict of interest.

References

1. Nielsen, M.A.; Chuang, I.L. *Quantum Computation and Quantum Information*; Cambridge University Press: Cambridge, UK, 2010.
2. Pirandola, S.; Andersen, U.L.; Banchi, L.; Berta, M.; Bunandar, D.; Colbeck, R.; Englund, D.; Gehring, T.; Lupo, C.; Ottaviani, C.; et al. Advances in quantum cryptography. *Adv. Opt. Photon.* **2020**, *12*, 1012. [[CrossRef](#)]
3. Wang, H.-W.; Tsai, C.-W.; Lin, J.; Huang, Y.-Y.; Yang, C.-W. Efficient and secure measure-resend authenticated semi-quantum key distribution protocol against reflecting attack. *Mathematics* **2022**, *10*, 1241. [[CrossRef](#)]
4. Zhu, Y.; Mao, L.; Hu, H.; Wang, Y.; Guo, Y. Adaptive continuous-variable quantum key distribution with discrete modulation regulative in free space. *Mathematics* **2022**, *10*, 4450. [[CrossRef](#)]
5. Bennett, C.H.; Brassard, G.; Crépeau, C.; Jozsa, R.; Peres, A.; Wootters, W.K. Teleporting an unknown quantum state via dual classical and Einstein-Podolsky-Rosen channels. *Phys. Rev. Lett.* **1993**, *70*, 1895. [[CrossRef](#)]
6. Horodecki, R.; Horodecki, M.; Horodecki, P. Teleportation, Bell's inequalities and inseparability. *Phys. Lett. A* **1996**, *222*, 21. [[CrossRef](#)]
7. Popescu, S. Bell's inequalities versus teleportation: What is nonlocality. *Phys. Rev. Lett.* **1994**, *72*, 797. [[CrossRef](#)] [[PubMed](#)]
8. Horodecki, M.; Horodecki, P.; Horodecki, R. General teleportation channel, singlet fraction, and quasidistillation. *Phys. Rev. A* **1999**, *60*, 1888. [[CrossRef](#)]
9. Verstraete, F.; Verschelde, H. Optimal teleportation with a mixed state of two qubits. *Phys. Rev. Lett.* **2003**, *90*, 097901. [[CrossRef](#)]

10. Bennett, C.H.; Wiesner, S.J. Communication via one- and two-particle operators on Einstein-Podolsky-Rosen states. *Phys. Rev. Lett.* **1992**, *69*, 2881. [[CrossRef](#)]
11. Barena, A.; Ekert, A. Dense coding based on quantum entanglement. *J. Mod. Opt.* **1995**, *42*, 1253. [[CrossRef](#)]
12. Mattle, K.; Weinfurter, H.; Kwiat, P.G.; Zeilinger, A. Dense coding in experimental quantum communication. *Phys. Rev. Lett.* **1996**, *76*, 4656. [[CrossRef](#)] [[PubMed](#)]
13. Hiroshima, T. Optimal dense coding with mixed state entanglement. *J. Phys. A Math. Gen.* **2001**, *34*, 6907. [[CrossRef](#)]
14. Bowen, G.; Bose, S. Teleportation as a depolarizing quantum channel, relative entropy, and classical capacity. *Phys. Rev. Lett.* **2001**, *87*, 267901. [[CrossRef](#)] [[PubMed](#)]
15. Alberverio, S.; Fei, S.M.; Yang, W.L. Optimal teleportation based on Bell measurements. *Phys. Rev. A* **2002**, *66*, 012301. [[CrossRef](#)]
16. Hu, M.L. Relations between entanglement, Bell-inequality violation and teleportation fidelity for the two-qubit X states. *Quantum Inf. Process.* **2013**, *12*, 229. [[CrossRef](#)]
17. Horodecki, M.; Piani, M. On quantum advantage in dense coding. *J. Phys. A Math. Theor.* **2012**, *45*, 105306. [[CrossRef](#)]
18. Hu, M.L.; Hu, X.; Wang, J.C.; Peng, Y.; Zhang, Y.R.; Fan, H. Quantum coherence and geometric quantum discord. *Phys. Rep.* **2018**, *762–764*, 1–100. [[CrossRef](#)]
19. Lee, J.; Kim, M.S. Entanglement teleportation via Werner states. *Phys. Rev. Lett.* **2000**, *84*, 4236. [[CrossRef](#)]
20. Oh, S.; Lee, S.; Lee, H.W. Fidelity of quantum teleportation through noisy channels. *Phys. Rev. A* **2002**, *66*, 022316. [[CrossRef](#)]
21. Jung, E.; Hwang, M.R.; Ju, Y.H.; Kim, M.S.; Yoo, S.K.; Kim, H.; Park, D.; Son, J.W.; Tamaryan, S.; Cha, S.K. Greenberger–Horne–Zeilinger versus W states: Quantum teleportation through noisy channels. *Phys. Rev. A* **2008**, *78*, 012312. [[CrossRef](#)]
22. Bhaktavatsala Rao, D.D.; Panigrahi, P.K.; Mitra, C. Teleportation in the presence of common bath decoherence at the transmitting station. *Phys. Rev. A* **2008**, *78*, 022336.
23. Yeo, Y.; Kho, Z.W.; Wang, L. Effects of Pauli channels and noisy quantum operations on standard teleportation. *EPL* **2009**, *86*, 40009. [[CrossRef](#)]
24. Shadman, Z.; Kampermann, H.; Macchiavello, C.; Bruß, D. Optimal super dense coding over noisy quantum channels. *New J. Phys.* **2010**, *12*, 073042. [[CrossRef](#)]
25. Quek, S.; Li, Z. Effects of quantum noises and noisy quantum operations on entanglement and special dense coding. *Phys. Rev. A* **2010**, *81*, 024302. [[CrossRef](#)]
26. Li, J.K.; Xu, K.; Zhang, G.F. Dense coding capacity in correlated noisy channels with weak measurement. *Chin. Phys. B* **2021**, *30*, 110302. [[CrossRef](#)]
27. Haddadi, S.; Hu, M.L.; Knedif, Y.; Dolatkah, H.; Pourkarimi, M.R.; Daoud, M. Measurement uncertainty and dense coding in a two-qubit system: Combined effects of bosonic reservoir and dipole–dipole interaction. *Results Phys.* **2022**, *32*, 105041. [[CrossRef](#)]
28. Sun, Y.H.; Xie, Y.X. Memory effect of a dephasing channel on measurement uncertainty, dense coding, teleportation, and quantum Fisher information. *Results Phys.* **2022**, *37*, 105526. [[CrossRef](#)]
29. Yeo, Y. Teleportation with a mixed state of four qubits and the generalized singlet fraction. *Phys. Rev. A* **2006**, *74*, 052305. [[CrossRef](#)]
30. Yeo, Y. Local noise can enhance two-qubit teleportation. *Phys. Rev. A* **2008**, *78*, 022334. [[CrossRef](#)]
31. Laine, E.M.; Breuer, H.P.; Piilo, J. Nonlocal memory effects allow perfect teleportation with mixed states. *Sci. Rep.* **2014**, *4*, 4620. [[CrossRef](#)]
32. Guo, Y.N.; Tian, Q.L.; Zeng, K.; Chen, P.X. Fidelity of quantum teleportation in correlated quantum channels. *Quantum Inf. Process.* **2020**, *19*, 182. [[CrossRef](#)]
33. Hu, M.L.; Zhang, Y.H.; Fan, H. Nonlocal advantage of quantum coherence in a dephasing channel with memory. *Chin. Phys. B* **2021**, *30*, 030308. [[CrossRef](#)]
34. Li, Y.L.; Zu, C.J.; Wei, D.M. Enhance quantum teleportation under correlated amplitude damping decoherence by weak measurement and quantum measurement reversal. *Quantum Inf. Process.* **2019**, *18*, 2. [[CrossRef](#)]
35. Tian, M.B.; Zhang, G.F. Improving the capacity of quantum dense coding by weak measurement and reversal measurement. *Quantum Inf. Process.* **2018**, *17*, 19. [[CrossRef](#)]
36. Breuer, H.P.; Petruccione, F. *The Theory of Open Quantum Systems*; Oxford University Press: Oxford, UK, 2007.
37. Rivas, Á.; Huelga, S.F. *Open Quantum Systems. An Introduction*; Springer: Berlin/Heidelberg, Germany, 2012.
38. Cai, X.; Zheng, Y. Quantum dynamical speedup in a nonequilibrium environment. *Phys. Rev. A* **2017**, *95*, 052104. [[CrossRef](#)]
39. Cai, X.; Zheng, Y. Non-Markovian decoherence dynamics in nonequilibrium environments. *J. Chem. Phys.* **2018**, *149*, 094107.
40. Cai, X. Quantum dephasing induced by non-Markovian random telegraph noise. *Sci. Rep.* **2020**, *10*, 88. [[CrossRef](#)]
41. Czerwinski, A. Quantum communication with polarization-encoded qubits under majorization monotone dynamics. *Mathematics* **2022**, *10*, 3932. [[CrossRef](#)]
42. Breuer, H.P.; Laine, E.M.; Piilo, J. Measure for the degree of non-Markovian behavior of quantum processes in open systems. *Phys. Rev. Lett.* **2009**, *103*, 210401. [[CrossRef](#)]
43. Breuer, H.P.; Laine, E.M.; Piilo, J.; Vacchini, B. Colloquium: Non-Markovian dynamics in open quantum systems. *Rev. Mod. Phys.* **2016**, *88*, 021002. [[CrossRef](#)]
44. Chen, H.; Han, T.; Chen, M.; Ren, J.; Cai, X.; Meng, X.; Peng, Y. Quantum state tomography in nonequilibrium environments. *Photonics* **2023**, *10*, 134. [[CrossRef](#)]

45. Werlang, T.; Souza, S.; Fanchini, F.F.; Villas Boas, C.J. Robustness of quantum discord to sudden death. *Phys Rev. A* **2009**, *80*, 024103. [[CrossRef](#)]
46. Xu, J.S.; Li, C.F.; Zhang, C.J.; Xu, X.Y.; Zhang, Y.S.; Guo, G.C. Experimental investigation of the non-Markovian dynamics of classical and quantum correlations. *Phys Rev. A* **2010**, *82*, 042328. [[CrossRef](#)]
47. Altintas, F.; Eryigit, R. Dissipative dynamics of quantum correlations in the strong-coupling regime. *Phys. Rev. A* **2013**, *87*, 022124. [[CrossRef](#)]
48. Czerwinski, A. Dynamics of open quantum systems—Markovian semigroups and beyond. *Symmetry* **2022**, *14*, 1752. [[CrossRef](#)]
49. Haddadi, S.; Pourkarimi, M.R.; Wang, D. Tripartite entropic uncertainty in an open system under classical environmental noise. *J. Opt. Soc. Am. B* **2021**, *38*, 2620. [[CrossRef](#)]
50. Pourkarimi, M.R.; Haseli, S.; Haddadi, S.; Hadipour, M. Scrutinizing entropic uncertainty and quantum discord in an open system under quantum critical environment. *Laser Phys. Lett.* **2022**, *19*, 065201. [[CrossRef](#)]
51. Rahman, A.U.; Haddadi, S.; Javed, M.; Kenfack, L.T.; Ullah, A. Entanglement witness and linear entropy in an open system influenced by FG noise. *Quantum Inf. Process.* **2022**, *21*, 368. [[CrossRef](#)]
52. Rahman, A.U.; Ali, H.; Haddadi, S.; Zangi, S.M. Generating non-classical correlations in two-level atoms. *Alex. Eng. J.* **2023**, *67*, 425. [[CrossRef](#)]
53. Yu, T.; Eberly, J.H. Finite-time disentanglement via spontaneous emission. *Phys. Rev. Lett.* **2004**, *93*, 140404. [[CrossRef](#)]
54. Almeida, M.P.; de Melo, F.; Hor-Meyll, M.; Salles, A.; Walborn, S.P.; Souto Ribeiro, P.H.; Davidovich, L. Environment-induced sudden death of entanglement. *Science* **2007**, *316*, 579. [[CrossRef](#)]
55. Yu, T.; Eberly, J.H. Sudden death of entanglement. *Science* **2009**, *323*, 5914. [[CrossRef](#)] [[PubMed](#)]
56. Bellomo, B.; Lo Franco, R.; Compagno, G. Non-Markovian effects on the dynamics of entanglement. *Phys. Rev. Lett.* **2007**, *99*, 160502. [[CrossRef](#)] [[PubMed](#)]
57. Chen, M.; Chen, H.; Han, T.; Cai, X. Disentanglement Dynamics in Nonequilibrium Environments. *Entropy* **2022**, *24*, 1330. [[CrossRef](#)]
58. Czerwinski, A. Entanglement dynamics governed by time-dependent quantum generators. *Axioms* **2022**, *11*, 589. [[CrossRef](#)]
59. Kim, Y.S.; Lee, J.C.; Kwon, O.; Kim, Y.H. Protecting entanglement from decoherence using weak measurement and quantum measurement reversal. *Nat. Phys.* **2012**, *8*, 117. [[CrossRef](#)]
60. Lidar, D.A.; Birgitta Whaley, K. *Decoherence-Free Subspaces and Subsystems. Irreversible Quantum Dynamics*; Benatti, F., Floreanini, R., Eds.; Springer: Berlin/Heidelberg, Germany, 2003.
61. Flores M.M.; Galapon E.A. Two qubit entanglement preservation through the addition of qubits. *Ann. Phys.* **2015**, *354*, 21. [[CrossRef](#)]
62. Morteza pour, A.; Ahmadi Borji, M.; Lo Franco, R. Protecting entanglement by adjusting the velocities of moving qubits inside non-Markovian environments. *Laser Phys. Lett.* **2017**, *14*, 055201. [[CrossRef](#)]
63. Haas, M.; Jentschura, U.D.; Keitel, C.H.; Kolachevsky, N.; Herrmann, M.; Fendel, P.; Fischer, M.; Udem, T.; Holzwarth, R.; Hänsch, T.W.; et al. Two-photon excitation dynamics in bound two-body Coulomb systems including ac Stark shift and ionization. *Phys. Rev. A* **2006**, *73*, 052501. [[CrossRef](#)]
64. Agarwal, G.S.; Pathak, P.K. dc-field-induced enhancement and inhibition of spontaneous emission in a cavity. *Phys. Rev. A* **2004**, *70*, 025802. [[CrossRef](#)]
65. Ghosh, B.; Majumdar, A.S.; Nayak, N. Control of atomic entanglement by the dynamic Stark effect. *J. Phys. B At. Mol. Opt. Phys.* **2008**, *41*, 065503. [[CrossRef](#)]
66. Baghshahi, H.R.; Tavassoly, M.K.; Faghihi, M.J. Entanglement analysis of a two-atom nonlinear Jaynes–Cummings model with nondegenerate two-photon transition, Kerr nonlinearity, and two-mode Stark shift. *Laser Phys.* **2014**, *24*, 125203. [[CrossRef](#)]
67. Golkar, S.; Tavassoly, M.K. Dynamics and maintenance of bipartite entanglement via the Stark shift effect inside dissipative reservoirs. *Laser Phys. Lett.* **2018**, *15*, 035205. [[CrossRef](#)]
68. Puri R.R.; Bullough, R.K. Quantum electrodynamics of an atom making two-photon transitions in an ideal cavity. *J. Opt. Soc. Am. B* **1988**, *5*, 2021. [[CrossRef](#)]
69. Spohn, H. Kinetic equations from Hamiltonian dynamics: Markovian limits. *Rev. Mod. Phys.* **1980**, *52*, 569. [[CrossRef](#)]
70. Dalton, B.J.; Barnett, S.M.; Garraway, B.M. Theory of pseudomodes in quantum optical processes. *Phys. Rev. A* **2001**, *64*, 053813. [[CrossRef](#)]
71. Yeo, Y. Teleportation via thermally entangled states of a two-qubit Heisenberg XX chain. *Phys. Rev. A* **2002**, *66*, 062312. [[CrossRef](#)]
72. Zhou, Y.; Zhang, G.F. Quantum teleportation via a two-qubit Heisenberg XXZ chain—effects of anisotropy and magnetic field. *Eur. Phys. J. D* **2008**, *47*, 227. [[CrossRef](#)]
73. Benabdallah, F.; Haddadi, S.; Arian Zad, H.; Pourkarimi, M.R.; Daoud, M.; Ananikian, N. Pairwise quantum criteria and teleportation in a spin square complex. *Sci. Rep.* **2022**, *12*, 6406. [[CrossRef](#)]
74. Liang, Y.C.; Yeh, Y.H.; Mendonça, P.E.M.F.; Teh, R.Y.; Reid, M.D.; Drummond P.D. Quantum fidelity measures for mixed states. *Rep. Prog. Phys.* **2019**, *82*, 076001. [[CrossRef](#)]
75. Rahman, A.U.; Haddadi, S.; Pourkarimi, M.R.; Ghominejad, M. Fidelity of quantum states in a correlated dephasing channel. *Laser Phys. Lett.* **2022**, *19*, 035204. [[CrossRef](#)]
76. Zidan, N.; Rahman, A.U.; Haddadi, S. Quantum teleportation in a two-superconducting qubit system under dephasing noisy channel: Role of Josephson and mutual coupling energies. *Laser Phys. Lett.* **2023**, *20*, 025204. [[CrossRef](#)]

77. Pourkarimi, M.R.; Haddadi, S. Quantum-memory-assisted entropic uncertainty, teleportation, and quantum discord under decohering environments. *Laser Phys. Lett.* **2020**, *17*, 025206. [[CrossRef](#)]
78. Schumacher, B.; Westmoreland, M.D. Sending classical information via noisy quantum channels. *Phys. Rev. A* **1997**, *56*, 131. [[CrossRef](#)]
79. Holevo, A.S. The capacity of the quantum channel with general signal states. *IEEE Trans. Inf. Theory* **1998**, *44*, 269. [[CrossRef](#)]
80. Haddadi, S.; Ghominejad, M.; Akhound, A.; Pourkarimi, M.R. Exploring entropic uncertainty relation and dense coding capacity in a two-qubit X-state. *Laser Phys. Lett.* **2020**, *17*, 095205. [[CrossRef](#)]
81. Abd-Rabbou, M.Y.; Khalil, E.M. Dense coding and quantum memory assisted entropic uncertainty relations in a two-qubit state influenced by dipole and symmetric cross interactions. *Ann. Phys.* **2022**, *534*, 2200204. [[CrossRef](#)]

Disclaimer/Publisher's Note: The statements, opinions and data contained in all publications are solely those of the individual author(s) and contributor(s) and not of MDPI and/or the editor(s). MDPI and/or the editor(s) disclaim responsibility for any injury to people or property resulting from any ideas, methods, instructions or products referred to in the content.